

Electric field controlled spin- and valley-polarized edge states in silicene with extrinsic Rashba effect

Zhiming Yu,¹ Hui Pan,² and Yugui Yao^{1,*}

¹*School of Physics, Beijing Institute of Technology, Beijing 100081, China*

²*Department of Physics, Beihang University, Beijing 100191, China*

(Dated: October 21, 2015)

In the presence of extrinsic Rashba spin-orbit coupling, we find that silicene can host a new quantum anomalous Hall state with spin- and valley-polarized edge states, which can be effectively controlled by the exchange field and electric field. In this new state, the pair of nontrivial edge states reside in one specific valley and have a strong but opposite spin polarization. A distinctive feature of this new state is that both of the spin and valley index of the edge states can be switched by reversing the electric field. We also present a microscopic mechanism for the origination of the new state. Our findings provide an efficient way to control the topologically protected spin- and valley-polarized edge states, which is crucial for spintronics and valleytronics.

PACS numbers: 73.43.-f, 71.70.Ej, 03.65.Vf, 72.25.-b

I. INTRODUCTION

Two dimensional topological insulators with honeycomb structure have attracted much attention due to various kinds of binary degree of freedom: spin, valley and sublattice¹⁻⁵, and the topologically protected metallic edge states^{6,7}. Nanoelectronic devices designed by topologically protected edge states are immune to the disorder and defects of system. Furthermore, these devices can take advantage of the intrinsic spin or valley degrees of freedom of system. Under some specific situations, the edge states of honeycomb materials are spin- or valley-polarized⁸. However, if these materials are planar such as graphene, the binary degree of freedom of the edge states are difficult to switch and thus cannot be applied in nanodevices. On the other hand, the electronic properties of low-buckled honeycomb materials can be tuned by electric field naturally.

Silicene, which is a low-buckled honeycomb material^{9,10}, exhibits various physical properties such as quantum spin Hall (QSH) effect⁹⁻¹², quantum anomalous Hall (QAH) effect¹³⁻¹⁵, strong circular dichroism¹⁶ and superconductivity^{17,18}. It also undergoes a topological phase transition by irradiating circular polarized light in the presence of electric field^{19,20}. Silicene has been synthesized on different substrates, including the surface of *Ag(111)*, *ZrB₂*, *In(111)* etc²¹⁻²⁴. Moreover, silicene field-effect transistor has been fabricated at room temperature recently²⁵.

Generally, the extrinsic Rashba spin-orbital coupling (SOC) of pristine silicene is zero because of the structure inversion symmetry¹⁰. And the extrinsic Rashba SOC induced by external electric field is negligible^{10,13}. But strong extrinsic Rashba SOC may arise due to metal-atom adsorption or substrate, as they break the structure inversion symmetry of system dramatically, as discussed in graphene²⁶⁻²⁹. Recently, the first-principles calculations have shown that the strong extrinsic SOC effect in silicene with adsorption of different transition

metal atoms attributes $\sim 7 - 44$ meV to the band gap³⁰, which is much larger than the gap (1.55 meV) of pristine silicene⁹. The ferromagnetic substrate and transition metal adatoms also can induce sizable exchange field^{31,32}.

In this work, we present that silicene with extrinsic Rashba SOC can host a new topological state in the space of exchange field and electric field: spin- and valley-polarized QAH insulator (SV-QAHI), possessing a nonzero Chern number $C = \pm 1$ and a pair of nontrivial edge states localized at a specific valley with a strong but opposite spin polarization. This new state is different from the valley-polarized QAH (VQAHI) insulator reported by Pan et. al.¹⁵, which is induced by the competition between intrinsic and extrinsic Rashba SOC. SV-QAHI can emerge without intrinsic Rashba SOC. A distinctive feature of SV-QAHI is that the spin and valley direction of the gapless edge states can be easily switched by reversing the electric field, resulting in an electric field control of spin and valley index. These switching properties of spin and valley index are useful for spintronics and valleytronics.

The present paper is composed as follows. In Sec. II, we introduce the tight-binding Hamiltonian of silicene with extrinsic Rashba SOC, exchange field and electric field. Section III presents the phase diagram of silicene in the space of exchange field and electric field. We also discuss the exotic properties and the origin of the nontrivial edge states of SV-QAHI in this section. Finally, we give our conclusion and summarize our results in Sec. IV.

II. HAMILTONIAN

The tight-binding (TB) Hamiltonian of silicene with extrinsic Rashba SOC, exchange field and electric field

reads¹⁰:

$$\begin{aligned}
 H = & -t \sum_{\langle i,j \rangle \alpha} c_{i\alpha}^\dagger c_{j\alpha} + i \lambda \sum_{\langle i,j \rangle \alpha\beta} c_{i\alpha}^\dagger (\boldsymbol{\sigma} \times \mathbf{d}_{ij})_{\alpha\beta}^z c_{j\beta} \\
 & + M \sum_{i\alpha\beta} c_{i\alpha}^\dagger \sigma_{\alpha\beta}^z c_{i\beta} + \Delta \sum_{i\alpha} \mu_i c_{i\alpha}^\dagger c_{i\alpha}
 \end{aligned} \quad (1)$$

where $c_{i\alpha}^\dagger$ ($c_{i\alpha}$) is the electronic creation (annihilation) operator with spin α at site i . $\boldsymbol{\sigma}$ is the Pauli matrix, \mathbf{d}_{ij} represents a unit vector connecting sites i and j , and $\langle i, j \rangle$ stands for nearest-neighbor sites. The first term is the usual nearest-neighbor hopping with $t = 1.08 \text{ eV}$ ¹⁰. The second and third terms represent the extrinsic Rashba SOC (λ) and exchange field (M) respectively, both can be induced by ferromagnetic substrate or adsorption of transition metal atoms on silicene³⁰. Δ is the staggered sublattice potential arising from an electric field perpendicular to silicene sheet. Here, we neglect the influence of electric field on extrinsic Rashba SOC. We also neglect the intrinsic SOC and intrinsic Rashba SOC, as the adatoms or substrate induced extrinsic Rashba SOC may be much stronger than the intrinsic SOC^{26,29,30}, in which situations we are interested.

III. PHASE DIAGRAM AND SPIN- AND VALLEY-POLARIZED EDGE STATES

In Fig. 1, we presented the phase diagram of silicene in the (M, Δ) space. All the phases are characterized by the Chern number (C) and the valley degree of freedom of the nontrivial edge states (V_{edge}). The Chern number (C) determines the topological properties of phase. And V_{edge} is introduced to present the valley-polarized properties of the nontrivial edge states. We define $V_{edge} \equiv 1/-1$ when the gapless edge states are localized around K/K' valley, and $V_{edge} \equiv 0$ if there is no gapless edge states or the gapless edge states are not localized around one specific valley. When exchange field dominates over the electric field, silicene is a quantum anomalous Hall insulator (QAHI) with $(C, V_{edge}) = (2, 0)$ for $M > 0$. In Fig. 2, we present the band structures of the zigzag-terminated nanoribbon at marked points in Fig. 1. The nanoribbon band structure of QAHI with $(C, V_{edge}) = (2, 0)$ is presented in Fig. 2b. Silicene undergoes a topological phase transition from QAHI to SV-QAHI when the strength of external electric field increases and crosses a critical value. The index of SV-QAHI is $(-1, 1)$ for $M > 0$ and $\Delta > 0$, as shown in Fig. 2a. Keep increasing the electric field, silicene would undergo another topological phase transition to a band insulator (BI) with index $(0, 0)$.

The most exciting finding is that the edge states of zigzag-terminated SV-QAHI are approximately mono-component, and the spin and valley direction of them can be switched by electric field. For clarity, we define the uppermost/downmost atoms of the zigzag-terminated nanoribbon belong to sublattice A/B. Let us start from SV-QAHI with index $(-1, 1)$ ($\Delta > 0$ & $M > 0$), of which

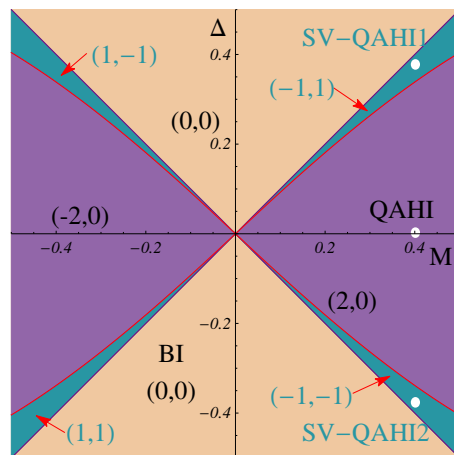


FIG. 1. (Color online) Phase Diagram of silicene in the (M, Δ) space with extrinsic Rashba SOC $\lambda = 0.2 t$, calculated from the TB Hamiltonian (1). The solid lines separate the phases, which are indexed by the Chern number and the valley index of the edge state (C, V_{edge}) . We define $V_{edge} \equiv 1/-1$ when the gapless edge states are located around K/K' valley, and $V_{edge} \equiv 0$ if there is no gapless edge state or the gapless edge states are not located around one valley. M and Δ are in unit of t .

the edge currents at the top- and bottom-edge of nanoribbon are mainly composed by $|A, K, \downarrow\rangle$ and $|B, K, \uparrow\rangle$ respectively, as shown in Fig. 3a. If we reverse the electric field and keep exchange field unchanged ($\Delta < 0$ & $M > 0$), silicene becomes a $(-1, -1)$ SV-QAHI (Fig. 3b), and the binary indices of top- and bottom-edge states become $|A, K', \uparrow\rangle$ and $|B, K', \downarrow\rangle$, directly demonstrating that the spin and valley index of the edge states have been switched. And if we reverse the exchange field instead of electric field ($\Delta > 0$ & $M < 0$), silicene turns into $(1, -1)$ SV-QAHI (Fig. 3c), and the binary indices of top- and bottom-edge states become $|A, K', \uparrow\rangle$ and $|B, K', \downarrow\rangle$ respectively which are same as that of $(-1, -1)$ SV-QAHI (Fig. 3b). But the direction of top- and bottom-edge current between $(1, -1)$ and $(-1, -1)$ SV-QAHI are opposite, which can be found by the Chern numbers and the slopes of the edge states of these two insulators. Similarly, the binary indices of the edge currents of $(1, 1)$ SV-QAHI (Fig. 3d) are the same as that of $(-1, 1)$ SV-QAHI (Fig. 3a), while the direction of edge currents of them are opposite too. In short, we can switch the polarization direction of spin and valley of the edge states by reversing electric field. And the polarization direction of spin, valley and the propagation of edge current are all switched by reversing exchange field.

In order to understand the underlying physics of SV-QAHI, we first explore the phase diagram of silicene analytically by a low-energy effective Hamiltonian³³, then discuss the origination of the approximately mono-component edge states, and the electric field control of spin and valley direction of the edge states. First, we expand the TB Hamiltonian (1) around valley points (K

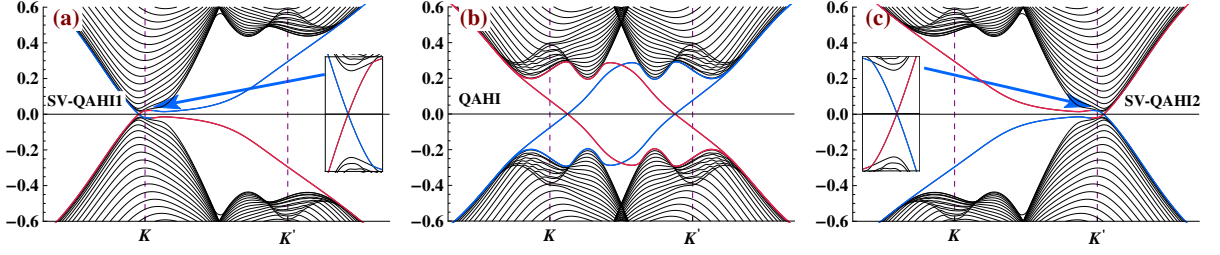


FIG. 2. (Color online) Band structures of the zigzag-terminated nanoribbon at marked points in Fig. 1, calculated from the TB Hamiltonian (1). The topological index (\mathcal{C}, V_{edge}) are (a) SV-QAHI1: $(1, 1)$ ($\Delta = 0.38 t$ & $M = 0.4 t$); (b) QAHI: $(2, 0)$ ($\Delta = 0 t$ & $M = 0.4 t$); (c) SV-QAHI2: $(1, -1)$ ($\Delta = -0.38 t$ & $M = 0.4 t$). Blue/Red curves represents edge states propagating along the top/bottom edge of nanoribbon. Energy is in unit of t and momentum is in unit of $1/a$.

and K'):

$$H^\tau = \begin{pmatrix} \Delta + M & h_+ & 0 & -v_F k_+^\tau \\ h_+^* & -\Delta - M & -v_F k_+^\tau & 0 \\ 0 & -v_F k_+^\tau & \Delta - M & h_- \\ -v_F k_-^\tau & 0 & h_-^* & -\Delta + M \end{pmatrix} \quad (2)$$

with the basis $(A \uparrow, B \downarrow, A \downarrow, B \uparrow)^T$, and

$$h_\pm = i\frac{3}{2}\lambda(1 \pm \tau) - \frac{\sqrt{3}}{4}\lambda(\tau \mp 1)(ik_x + \tau k_y) a \quad (3)$$

where $\tau = \pm 1$ represents valley degrees of freedom $K(K')$, and $k_\pm^\tau = \tau k_x \pm ik_y$. $v_F = \frac{\sqrt{3}}{2}at = 5.5 \times 10^5 m/s$ is Fermi velocity with the lattice constant $a = 3.86 \text{ \AA}^{10}$. Since the extrinsic Rashba SOC is not negligible in the present model, we keep $\lambda k_{x(y)}$ in the second term of Eq. (3), and it turns out that $\lambda k_{x(y)}$ is crucial to obtain the SV-QAHI, and leads to the trigonal warping effects around the valleys. As shown in Eq. (3), the extrinsic Rashba SOC term is strongly valley dependent, and couples $|A \uparrow\rangle(|A \downarrow\rangle)$ and $|B \downarrow\rangle(|B \uparrow\rangle)$ as to make the spin and sublattice degrees of freedom are tightly connected to each other. Therefore, the operations on sublattice potential by electric field would affect the spin, which gives rise to a possibility of full electric-field control of spin of the system.

The energy bands of silicene at K or K' points are $\pm(\Delta + M)$ and $\pm\sqrt{(M - \Delta)^2 + 9\lambda^2}$ or $\pm(\Delta - M)$ and $\pm\sqrt{(M + \Delta)^2 + 9\lambda^2}$, respectively. When Δ approaches M , the low-energy bands ($\pm(|\Delta| - |M|)$) are well separated from the other high-energy bands ($\pm\sqrt{(|M| - |\Delta|)^2 + 9\lambda^2}$) owing to nonzero λ . Thus, in the presence of extrinsic Rashba SOC and $|\Delta| \simeq |M|$, a two-band low energy effective Hamiltonian can be established¹⁰:

$$H_{eff}(\mathbf{k}) = \mathbf{d}(\mathbf{k}) \cdot \boldsymbol{\sigma} \quad (4)$$

with

$$\begin{aligned} d_x &= -\lambda k_y a \left(\frac{\sqrt{3}}{2} + 3\eta\Gamma k_x/a \right) \\ d_y &= \frac{\sqrt{3}\lambda}{2} \left(\eta k_x a - \sqrt{3}\Gamma(k_x^2 - k_y^2) \right) \\ d_z &= \Delta - \eta M (1 - \Gamma k^2) \end{aligned}$$

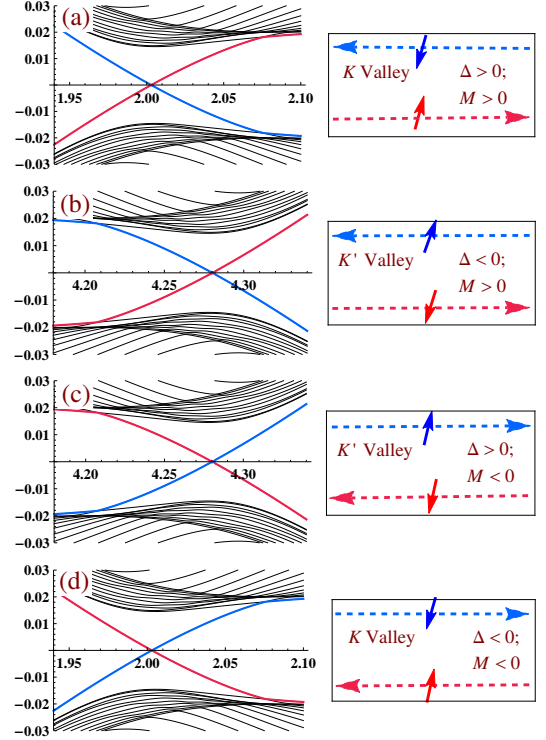


FIG. 3. (Color online) Enlarged edge states of zigzag-terminated nanoribbons of SV-QAHI in the four quadrant of (M, Δ) space. Strong spin polarization edge currents propagate along the nanoribbons edges. Blue/Red curves represents edge states propagating along the top/bottom edge of nanoribbon. By reversing the external electric field (Δ) or exchange field (M), the polarization direction of spin and valley of the edge states can be switched.

where $\eta = \text{Sgn}(M\Delta)$ and $\Gamma = 2v_F^2/(4|\Delta M| + 9\lambda^2)$. When $\eta = 1/-1$, the low-energy states are localized around K/K' valley, as shown in Fig. 3. The basis of $H_{eff}(\mathbf{k})$ is $(A \downarrow, B \uparrow)^T$ when $\eta = 1$ and $(A \uparrow, B \downarrow)^T$ when $\eta = -1$. The effective Hamiltonian also satisfies the fol-

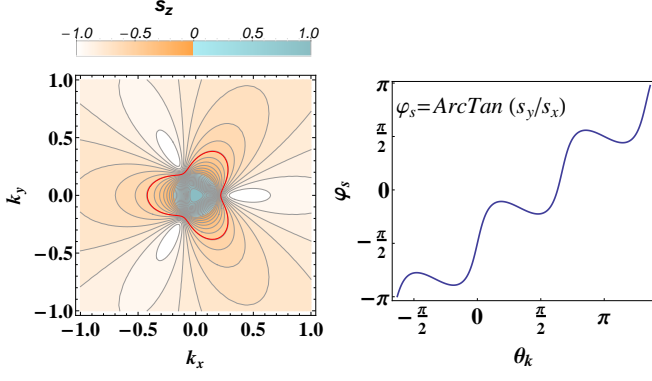


FIG. 4. (Color online) Skymion spin texture needs s_z ranges from 1 to -1 and the azimuth angle of spin $\varphi_s = \text{ArcTan}(s_y(\mathbf{k})/s_x(\mathbf{k}))$ changes from 0 to 2π with any s_z . Left: The contour map of s_z around K valley of SV-QAHI for $M > 0$ and $\Delta > 0$, calculated from the effective Hamiltonian $H_{eff}(\mathbf{k})$ (4), which shows the reversal of spin and the trigonal warping effect around valley. Right: Along the isoline of $s_z(\mathbf{k})$, the azimuth angle of spin φ_s changes from 0 to 2π . Here we present the behavior of φ_s as a function of $\theta_k = \text{ArcTan}(k_y/k_x)$ with $s_z(\mathbf{k}) = -0.6$. The isoline of $s_z(\mathbf{k}) = -0.6$ is marked by red curve in left figure. With other $s_z(\mathbf{k})$, φ_s also presents similar behavior (not shown). Hence, these two figures directly indicate that $H_{eff}(\mathbf{k})$ generates a Skymion spin texture.

lowing symmetry operations,

$$H_{eff}(-\Delta, M, \mathbf{k}) = \sigma_y H_{eff}(\Delta, M, -\mathbf{k}) \sigma_y \quad (5)$$

$$H_{eff}(-\Delta, -M, k_y) = \sigma_y H_{eff}(\Delta, M, -k_y) \sigma_y \quad (6)$$

Based on these symmetry operations, we can assume $\Delta > 0$ and $M > 0$ in the following discussion without loss of generality. The energy spectrum can be directly derived as $\varepsilon_{\mathbf{k}} = \pm|\mathbf{d}|$. The zero energy $\varepsilon_{\mathbf{k}} = 0$ only occurs when all the elements of $H_{eff}(\mathbf{k})$ vanish. We obtain two phase boundaries: $\Delta_+(M) = M$ with single Dirac point located at K point ($\mathbf{k}_+ = 0$), and

$$\Delta_-(M) = M \frac{6v_F^2 - 9\lambda^2 a^2}{6v_F^2 + 4M^2 a^2} \quad (7)$$

with three Dirac points located at

$$\mathbf{k}_- = k_- e^{in\pi/3} = \frac{a(4|\Delta_- M| + 9\lambda^2)}{2\sqrt{3}v_F^2} e^{in\pi/3} \quad (8)$$

with $n = 0, \pm 1$ corresponding to the trigonal warping terms. The SV-QAHI exists over the electric field region $\Delta_- < \Delta < \Delta_+$. Note that $H_{eff}(\mathbf{k})$ is only well defined around the valley centers, hence, $\Delta_-(M)$ (Eq. (7)) would be invalid when λ or M is large, where k_- (Eq. (8)) is large too. However, SV-QAHI does emerge when Δ is smaller than M and larger than a critical value, which can be found by the calculations of TB Hamiltonian (1).

Now we study the physical properties of the gapless edge states of SV-QAHI by the effective Hamiltonian

$H_{eff}(\mathbf{k})$. Generally, the topological properties of system can also be understood by Skymion spin (sublattice) texture^{34,35}. In Fig. 4, we present the contour map of z-component spin (sublattice) ($s_z(\mathbf{k})$) of SV-QAHI in the vicinity of Fermi level. $s_z(\mathbf{k}) = \langle v_k | \sigma_z | v_k \rangle$ with $|v_k\rangle = \frac{1}{N_k} (d_z - |\mathbf{d}|, d_x + id_y)^T$ being the eigenfunction of valence band of $H_{eff}(\mathbf{k})$ and N_k the normalization constant. The expression of $s_z(\mathbf{k})$ is too long and not necessary to present here. The important things are that in the SV-QAHI phase, $s_z(\mathbf{k} = 0) = 1$ and $s_z(\mathbf{k}') = -1$ with $\mathbf{k}' = a e^{in\pi/3} / (\sqrt{3}\Gamma(\Delta))$ and $n = 0, \pm 1$. Along the isoline of $s_z(\mathbf{k})$, the azimuth angle of spin $\varphi = \text{ArcTan}(s_y(\mathbf{k})/s_x(\mathbf{k}))$, changes from 0 to 2π continuously, which is shown in Fig. 4 too. Therefore a Skymion spin (sublattice) texture is generated in the SV-QAHI phase.

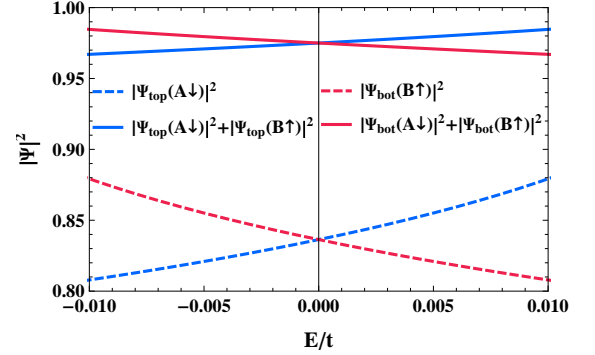


FIG. 5. (Color online) The probability of $|A \downarrow\rangle$ and $|B \uparrow\rangle$ in the edge states of zigzag-terminated SV-QAHI nanoribbon ($M > 0$ and $\Delta > 0$), obtained from the TB Hamiltonian (1). The solid lines intuitively show the edge states are almost composed by the basis of $H_{eff}(\mathbf{k})$: $(A \downarrow, B \uparrow)^T$. The dash lines show that the edge current propagating along top and bottom edge have strong spin polarization: mainly composed by $|A \downarrow\rangle$ and $|B \uparrow\rangle$ respectively.

Usually, Skymion and nontrivial edge states are two sides of the topological properties of system. Thus, the nontrivial edge states of nanoribbon can be expected to be mainly composed by $|A \downarrow\rangle$ and $|B \uparrow\rangle$, which are the basis of the low-energy effective Hamiltonian $H_{eff}(\mathbf{k})$. Fig. 5 presents the probability of $|A \downarrow\rangle$ and $|B \uparrow\rangle$ in the gapless edge states within the bulk energy gap. It shows that the total probability of $|A \downarrow\rangle$ and $|B \uparrow\rangle$ in the edge states is more than 96% (solid curves in Fig. 5). And the top/bottom edge current is mainly composed by $|A \downarrow\rangle/|B \uparrow\rangle$ (dashed curves in Fig. 5). From the effective Hamiltonian $H_{eff}(\mathbf{k})$, we know that if we reverse the electric field, the position of low-energy states changes from K valley to K' valley and the basis of $H_{eff}(\mathbf{k})$ changes from $(A \downarrow, B \uparrow)^T$ to $(A \uparrow, B \downarrow)^T$. Consequently, by reversing electric field, the component of the edge current propagating along the top/bottom-edge changes from $|A \downarrow\rangle/|B \uparrow\rangle$ to $|A \uparrow\rangle/|B \downarrow\rangle$, resulting in the electric field switching of spin and valley direction of the edge states.

At last, we make some discussions on the realization of SV-QAHI. From the effective Hamiltonian $H_{eff}(\mathbf{k})$ (4), we note that the SV-QAHI can exist over a wide electric field region when M or λ is large. Hence, the SV-QAHI may appear and be observed in silicene with suitable adsorption of transition metal atoms and ferromagnetic substrate. Moreover, since germanene and stanene share most of the electronic properties of silicene, we expect this SV-QAHI also can emerge in these two materials³⁶.

IV. CONCLUSIONS

In summary, we present that a new quantum anomalous Hall state can be obtained in silicene with extrinsic Rashba SOC. The gapless edge states of a zigzag-terminated nanoribbon of this new state have strong but opposite spin polarization and are located around one specific valley. The emergence of the novel spin- and valley-polarized edge states are explained in detail by two

band low-energy effective Hamiltonian model. It is found that the extrinsic Rashba SOC is crucial for realizing such new states. Particularly, the direction of spin and valley of the edge states can be easily switched by reversing the electric field or exchange field. This electric field control of spin and valley provides an opportunity to design newly topological-state based spintronic and valleytronic devices.

ACKNOWLEDGMENTS

We are thankful to Shengyuan A. Yang for revising this manuscript. This work was supported by the MOST Project of China (Grants Nos. 2014CB920903, and 2011CBA00100), the NSFC (Grants Nos. 11174022, 11174337, 11225418, 61227902, and 11574029), and the Specialized Research Fund for the Doctoral Program of Higher Education of China (Grant No. 20121101110046).

-
- * yg Yao@bit.edu.cn
- ¹ F. D. Haldane, Phys. Rev. Lett. 61, 2015 (1988).
 - ² D. Xiao, W. Zhu, Y. Ran, N. Nagaosa, and S. Okamoto, Nat. Comm. 2, 596(2011).
 - ³ Y. Xu, B. H. Yan, H. J. Zhang, J. Wang, G. Xu, P. Z. Tang, W. H. Duan, and S.-C. Zhang, Phys. Rev. Lett. 111, 136804(2013).
 - ⁴ Z. Song, C.-C. Liu, J. Yang, J. Han, M. Ye, B. Fu, Y. Yang, Q. Niu, J. Lu, and Y. G. Yao, NPG Asia Materials 6, e147(2014).
 - ⁵ C.-C. Liu, S. Guan, Z. Song, S. A. Yang, J. Yang, and Y. Yao, Phys. Rev. B 90, 085431(2014).
 - ⁶ M. Z. Hasan and C. Kane, Rev. Mod. Phys. 82, 3045(2010).
 - ⁷ X.-L. Qi and S.-C. Zhang, Rev. Mod. Phys. 83, 1057(2011).
 - ⁸ Z.H. Qiao, W.-K. Tse, H. Jiang, Y.G. Yao, and Q. Niu, Phys. Rev. Lett. 107, 256801 (2011).
 - ⁹ C.-C. Liu, W. Feng, and Y. G. Yao, Phys. Rev. Lett. 107, 076802(2011).
 - ¹⁰ C.-C. Liu, H. Jiang, and Y. G. Yao, Phys. Rev. B 84, 195430(2011).
 - ¹¹ C. L. Kane, and E. J. Mele, Phys. Rev. Lett. 95, 146802(2005).
 - ¹² C. L. Kane, and E. J. Mele, Phys. Rev. Lett. 95, 226801 (2005).
 - ¹³ M. Ezawa, Phys. Rev. Lett. 109, 055502 (2012).
 - ¹⁴ M. Ezawa, Phys. Rev. B 87, 155415(2013).
 - ¹⁵ H. Pan, Z. Li, C.-C. Liu, G. Zhu, Z. H. Qiao, and Y. G. Yao, Phys. Rev. Lett. 112, 106802 (2014).
 - ¹⁶ M. Ezawa, Phys. Rev. B 86, 161407 (2012).
 - ¹⁷ W.H. Wan, Y.F. Ge, F. Yang and Y.G. Yao, Europhys. Lett. 104 36001;
 - ¹⁸ F. Liu, C.-C. Liu, K. Wu, F. Yang, and Y.G. Yao, Phys. Rev. Lett. 111, 066804 (2013).
 - ¹⁹ M. Ezawa, Phys. Rev. Lett. 110, 026603(2013).
 - ²⁰ A. Lopez, A. Scholz, B. Santos, and J. Schliemann, Phys. Rev. B 91.125105(2015).
 - ²¹ P. Vogt, P. Padova, C. Quaresima, et al, Phys. Rev. Lett. 108, 155501 (2012).
 - ²² A. Fleurence, R. Friedlein, T. Ozaki, et al, Phys. Rev. Lett. 108, 245501 (2012).
 - ²³ L. Chen, C.-C. Liu, B. Feng, X. et al, Phys. Rev. Lett. 109, 056804(2012).
 - ²⁴ L. Meng, Y. Wang, L. Zhang, et al, Nano. Lett. 13, 685(2013).
 - ²⁵ L. Tao, E. Cinquanta, D. Chiappe, C. Grazianetti, M. Fanciulli, M. Dubey, A. Molle and D. Akinwande, Nat. Nanotech. 10, 227(2015).
 - ²⁶ Y. S. Dedkov, M. Fomin, U. Rüdiger, and C. Laubschat, Phys. Rev. Lett. 100, 107602 (2008).
 - ²⁷ W. K. Tse, Z. Qiao, Y. Yao, A. H. MacDonald, and Q. Niu, Phys. Rev. B 83, 155447 (2011).
 - ²⁸ J. Ding, Z. Qiao, W. Feng, Y. Yao, and Q. Niu, Phys. Rev. B 84, 195444 (2011).
 - ²⁹ Z. H. Qiao, S. A. Yang, W. X. Feng, W.-K. Tse, J. Ding, Y. G. Yao, J.Wang, and Q. Niu, Phys. Rev. B 82, 161414 (2010).
 - ³⁰ Z. Ni, H. Zhong, X. Jiang, R. Quhe, G. Luo, Y. Wang, M. Ye, J. Yang, J. Shi and J. Lu, Nanoscale. 6, 7609(2014).
 - ³¹ X.-L. Zhang, L.-F. Liu and W.-M. Liu, Sci. Rep. 3, 2908(2013).
 - ³² T. P. Kaloni, N. Singh, and U. Schwingenschlogl, Phys. Rev. B. 89, 035409(2014).
 - ³³ S. Nakajima, Adv. Phys, 4, 363 (1953).
 - ³⁴ Z. H. Qiao, H. Jiang, X. Li, Y. G. Yao, and Q. Niu, Phys. Rev. B, 85, 115439 (2012).
 - ³⁵ H. Pan, X. Li, H. Jiang, Y. Yao, and S. A. Yang, Phys. Rev. B, 91, 045404(2015).
 - ³⁶ T. P. Kaloni, J. Phys. Chem. C, 118, 25200(2014).